Effect of projected band gap on neutralization of Cs ions during grazing scattering from a Cu(111) surface

A. G. Borisov
Laboratoire des Collisions Atomiques et Moléculaires, Unité Mixte de Recherche CNRS—Université Paris-Sud, UMR 8625, Bâtiment 351, 91405 Orsay Cedex, France

A. Mertens, S. Wethekam, and H. Winter
Institut für Physik der Humboldt-Universität zu Berlin, Brook-Taylor-Straße 6, D-12489 Berlin-Adlershof, Germany
(Received 14 February 2003; published 11 July 2003)

Cs ions with energies ranging from 10 keV to 1.8 MeV are scattered under a grazing angle of incidence from a flat and clean Cu(111) surface. The observed fractions of Cs atoms in the scattered beams and their dependence on projectile velocity are well described by a model of kinematically assisted resonant charge transfer between projectile and two-dimensional surface-state continuum of the target surface. A comparison with calculations for a target represented by the electronic structure of a free-electron metal shows neutral fractions which are enhanced for the Cu(111) by more than one order of magnitude. This is the strongest effect of the projected band gap of a metal surface on the charge transfer observed so far.

DOI: 10.1103/PhysRevA.68.012901 PACS number(s): 79.20.Rf, 34.50.Dy

I. INTRODUCTION

Charge transfer plays an important role in the interactions of atoms with solids and their surfaces as manifested by, e.g., its relevance for adsorption phenomena or for a variety of surface analytical tools [1]. As a consequence, considerable interest in this subject has been devoted to fundamental research as well as technological applications. Basic features of electron-transfer processes between atomic projectiles and solid targets can be well understood in the framework of simple models, where the binding energies of relevant atomic levels and of electrons in the solid (work function, Fermi energy) primarily determine the interaction scenario [2–4]. As prominent examples we mention here the ionization of alkali-metal atoms in front of metal surfaces via one-electron resonant tunneling (''resonant charge transfer,'' RCT) and the neutralization of noble-gas ions via the Auger transfer (''Auger neutralization,'' AN) involving two electrons.

In their pioneering studies, Hagstrum [5] and Los and Geerlings [3] provided basic concepts for a microscopic understanding of the interaction mechanisms, supported in recent years by model calculations on electronic transition rates for RCT [6–8] and AN [9,10] which result in a description of electron-transfer processes and the collision dynamics free from adjustable parameters. As a consequence, we note that, e.g., the neutralization of alkali-metal ions during impact on a metal surface with a ''simple'' electronic structure can be described nowadays on a quantitative level [11]. Essential aspects of the theoretical approach are based on (1) the free-electron gas (''jellium'') approximation for the description of the electronic structure of the target surface, (2) the image shift of the projectile levels in front of the surface, (3) the incorporation of kinematic effects in terms of a frame transformation (visualization of the Galilei transformation by the concept of a shifted Fermi sphere in momentum space [3,12]), (4) the incorporation of many-body aspects of RCT associated with the electronic structure of the projectile by inclusion of statistical factors for electron capture and loss processes [13,14].

These concepts have been successfully applied in quite a few cases and resulted in a reasonable description of experimental data obtained with metal targets where the jellium approach is not an adequate approximation for the electronic structure. However, recent studies with noble-metal surfaces showed clear deviations in this respect [15–17]. The electronic structure of the (111) faces of these metals shows a projected band gap in the direction of the surface normal (L gap) for their nearly free sp-electron band which extends from below the Fermi energy to vacuum energies. For the projectile states with energies lying within the projected band gap, RCT is strongly affected as compared to free-electron metal targets. This is because electrons cannot enter the surface along the direction of the surface normal, which is the preferential pathway of electron tunneling between projectile and surface because of the highest transparency of the potential barrier.

The ''wave-packet propagation'' (WPP) studies of the RCT in the case of the (111) noble-metal target surfaces [16–19] revealed specific new features in comparison to free-electron metal targets. It has been demonstrated that the RCT process has a pronounced nonadiabatic behavior with a projected band-gap effect depending on the collision velocity (interaction time) [18]. This prediction was confirmed in experiments on $H^{(-)}$ formation during scattering from Ag(111) and Ag(110) surfaces by Guillemot and Esaulov [15]. As a second important finding, the WPP studies revealed that the two-dimensional (2D) continuum of electronic states corresponding to electrons localized at the surface and moving parallel to it—the surface-state continuum—dominates RCT [16,17,19]. The effect of the 2D surface-state continuum was explored for the neutralization of alkali-metal ions [16] and formation of negative ions [16,17] during grazing scattering from a Cu(111) surface. In this case, the kinematic effects

arising from the frame transformation between projectile and surface have been used to ''probe'' the dimensionality of the continuum of the metal states involved in the RCT. These studies demonstrated in gross accord the theoretically predicted features, i.e., enhanced neutral or negative-ion fractions in the scattered beams, as compared to jellium targets, and a ''narrower'' kinematic resonance structure of these fractions as a function of the collision velocity.

The work presented here is a continuation of these investigations with Cs projectiles scattered under a grazing angle of incidence from a Cu(111) surface. After a brief outline of the theory, we will discuss experimental and calculated neutral atom fractions in the scattered beams, which show the largest effect of the projected *L*-band gap on charge exchange observed so far. A fair agreement between theory and experimental data provides clear evidence for dominant contributions of the 2D surface-state continuum to RCT. The special conditions for electron capture and loss in this case result in pronounced contributions of excited states in the formation of neutral atoms. Furthermore, from the comparison between calculations and measured data we find that the inelastic electron-electron interactions significantly contribute to the decay of the population of the projectile states. This feature is important, since RCT rates are strongly reduced as compared to the case for a free-electron metal surface [18,19].

II. THEORETICAL TREATMENT OF THE RESONANT CHARGE TRANSFER PROCESSES

The theoretical treatment of the RCT process between projectile and surface is based on the WPP method, detailed elsewhere [18–21]. This method consists of the direct solution of the nonstationary Schrödinger equation for the wave function $\Psi(t)$ of the outer (valence) electron of the Cs projectile active in the RCT. The time evolution is governed by the potential

$$V = V_{Cs^+} + V_S + \Delta V_S, \tag{1}$$

where V_{Cs^+} represents the electron interaction with projectile core [20], ΔV_S corresponds to the change of the electron-surface interaction due to the presence of the projectile core approximated by the classical image of the Cs^+ ion, and V_S is the electron interaction with the metal surface. Two descriptions for the metal surface are used. Within the jellium model, the electron-metal interaction potential is constant in the bulk, and joins asymptotically the image potential in vacuum [22]. The Cu(111) surface is described with a model potential given by Chulkov, Silkin, and Echenique [23], which takes into account the periodicity of the crystal in the direction of the surface normal. It reproduces gross features of the electronic structure of the *sp* band of Cu(111) relevant for our study. At the $\bar{\Gamma}$ point, we have a projected band gap extending from -5.91 eV to -0.75 eV with respect to the vacuum level, surface state (-5.305 eV), and image state (-0.815 eV). Both, the potential describing the free-electron metal and the Cu(111) model potential are only the functions of the electron coordinate *z* in the direction perpendicular to the surface. The electronic motion parallel to the surface is described by plane waves with a parabolic dispersion of the energy levels: $E(k_z, k_\parallel) = E(k_z) + k_\parallel^2/2$ (atomic units are used throughout the paper unless otherwise stated).

Direct charge transfer involving $3d$ electrons of Cu is not considered here. These electrons are well localized at Cu atomic cores so that they do not contribute to the final formation of atoms taking place several atomic units in front of the surface for grazing scattering (cf. ''freezing concept'' [3]). Furthermore, the binding energy of the $3d$ band with respect to the vacuum level is about 7–10 eV. This imposes already a large energy defect in charge transfer for the lowest $6s$ Cs orbital being bound by 3.89 eV for the free atom and enhanced further close to the surface via image charge interaction. Thus, charge transfer will be dominated by resonant transfer involving electrons from the *sp* band of Cu. We note that $3d$ electrons are implicitly included in our more rigorous treatment via the effective core approximation in the model potential [23] used to derive the electronic structure for the *sp* band of Cu.

We consider both, the static case where the projectile surface distance *Z* is fixed and the dynamic case where projectiles impinge onto the surface following a classical trajectory along the surface normal. In both cases, the system has cylindrical symmetry with respect to the *z* axis (surface normal through projectile center). The time-dependent wave function of the active electron is then described on a finite mesh in cylindrical coordinates (ρ, *z*):

$$\Psi \equiv \Psi_m(\rho, z; t). \tag{2}$$

The magnetic quantum number *m* is defined by the symmetry of the projectile state under study. The time propagation is performed by the split-operator technique [24,25] for given initial conditions $\Psi(t=0) \equiv \psi$. For the wave function ψ, we use wave functions of the ground $6s$ or excited $6p$ ($m=0, m=\pm 1$) states of the free Cs atom. Higher excited states were not considered here, since their populations in grazing scattering are assumed to be small [26–28] (see also discussion in Sec. III). In the static case, we extract the properties of the projectile states involved in charge transfer. These are the energies $E_i(Z)$, the widths $\Gamma_i(Z)$, and the probabilities $|\sigma_i(\vec{k}, Z)|^2$ of electron escape into a given state $\vec{k}$ of the metal continuum, where $i = [6s; 6p(m=0); 6p(s); 6p(a)]$ denote the projectile states. Here, we consider symmetric (*s*) and antisymmetric (*a*) combinations of Cs $6p(m=\pm 1)$ orbitals with respect to the scattering plane.

For grazing scattering geometry, the collision velocity component perpendicular to the surface ($v_\perp$) is small (up to some 10^{-2} a.u.). Then, the WPP approach shows that the evolution of the population of projectile states can be described by the rate equation approach [18,29,30]. On the other hand, the velocity component parallel to the surface is large, so that one has to take into account kinematic effects by a Galilei transformation between the projectile and the surface frame [12].

Within a multistate rate equation approach, the time evolution of the populations of projectile states is given by

$$\partial_t P_i = -\Gamma_i^l P_i + \Gamma_i^c P_+ ,$$

$$\partial_t P_+ = \sum_i \Gamma_i^l P_i - \left(\sum_i \Gamma_i^c \right) P_+ , \tag{3}$$

where P_i are populations of the different substates of the neutral projectile with total neutral fractions in the scattered beam given by $P_0 = \Sigma_i P_i$. P_+ is the positive-ion fraction, and Γ_i^l and $\Gamma_i{}^c$ are the corresponding loss and capture rates. The latter depend on the distance from the surface and on the projectile velocity component parallel to the surface. In grazing surface collisions, the ''memory'' of initial charge states is lost. We then solve Eqs. (3) on the outgoing path of a classical trajectory of the projectile. Initial conditions correspond to equilibrium populations at the starting point of integration.

Effects of the parallel velocity are incorporated via the shifted Fermi-sphere model [2–4,11,12,26]. For the 3D free-electron continuum (jellium metal target), the capture and loss rates are derived from [11,28]

$$\begin{Bmatrix} \Gamma_i^c(Z) \\ \Gamma_i^l(Z) \end{Bmatrix} = \Gamma_i(Z) \begin{Bmatrix} g^c \\ g^l \end{Bmatrix} \times \int_0^{2\pi} d\varphi \int_0^{\pi} \sin\theta d\theta |\sigma_i(\theta,\varphi,Z)|^2 \times \begin{cases} f((\vec{k}+\vec{\nu}_\parallel)^2/2) \\ 1 - f((\vec{k}+\vec{\nu}_\parallel)^2/2). \end{cases} \tag{4}$$

The metal state electron wave vector $\vec{k} = (k,\theta,\varphi)$ is expressed in spherical coordinates. It satisfies the resonance condition $k = \sqrt{2[E_i(Z) - U]}$, where U is the energy of the bottom of the conduction band; $g^c = 2$ and $g^l = 1$ are spin statistical factors; $|\sigma_i(\theta,\varphi,Z)|^2$ is the normalized distribution of the transition probability; and $f((\vec{k}+\vec{\nu}_\parallel)^2/2)$ is the modified Fermi-Dirac distribution in the projectile rest frame. For grazing scattering, symmetry is reduced to the scattering plane, and symmetric (s) and antisymmetric (a) combinations of Cs $6p(m=\pm 1)$ orbitals with respect to the scattering plane have to be considered. This leads to $\cos\varphi$ and $\sin\varphi$ dependencies of $\sigma_{6p(s)}(\theta,\varphi,Z)$ and $\sigma_{6p(a)}(\theta,\varphi,Z)$, respectively [11]. For the $6s$ and $6p(m=0)$ states, σ_i are independent of φ.

The interpretation of Eq. (4) is straightforward. Capture (loss) rates depend on the number of occupied (empty) metal levels in resonance with the atomic level. The phase space is weighted by the transition probability which is strongly peaked in the direction of the surface normal. Because of the low binding energies of the Cs levels relative to the target work function, capture rates are much smaller than loss rates, leading to very small neutral Cs fractions. The calculations using the jellium model are displayed in Fig. 4. Neutral fractions of typically 1% are predicted for the jellium-Cu surface. The width of the kinematic resonance structure for neutral Cs fractions is given by the diameter of the Fermi sphere ($2k_F$), $k_F = 0.72$ a.u. in the present case. Our calculations show that the neutral fractions in the scattered beam are dominated by the Cs($6s$) ground state, whereas contributions of excited states are negligibly small. This feature was already established in studies on alkali-metal atom formation during grazing scattering from an Al(111) surface [26–28,31]. The low populations of excited states result from their larger energy difference with respect to the Fermi level of the surface in comparison with the ground state. Then electron loss is strongly favored in comparison with electron capture, i.e., $\Gamma^c \ll \Gamma^l$.

The situation is different for the model Cu(111) surface. From WPP studies we find that the coupling of projectile states with the 2D surface-state continuum is about one order of magnitude stronger than with the 3D bulk continuum. In the model for Cu(111), the surface-state continuum corresponds to electrons moving freely parallel to the surface with energy $E = E_{SS} + k_\parallel^2/2$, $\vec{k}_\parallel = (k_\parallel \cos\varphi, k_\parallel \sin\varphi)$ being the 2D electron wave vector. Capture and loss rates for the 2D continuum are

$$\begin{Bmatrix} \Gamma_i^c(Z) \\ \Gamma_i^l(Z) \end{Bmatrix} = \Gamma_i(Z) \begin{Bmatrix} g^c \\ g^l \end{Bmatrix} \times \int_0^{2\pi} d\varphi |\sigma_i(\varphi)|^2 \times \begin{cases} f((\vec{k}+\vec{\nu}_\parallel)^2/2) \\ 1 - f((\vec{k}+\vec{\nu}_\parallel)^2/2), \end{cases} \tag{5}$$

where $k_\parallel$ is given by the resonance condition $k_\parallel = \sqrt{2[E_i(Z) - E_{SS}]}$.

Parallel-velocity-assisted charge transfer for a target represented by a 2D continuum clearly differs from that for a 3D continuum. The Fermi sphere shrinks to a Fermi disk. The only remaining angular variable is the azimuth φ. For the $6s$ and $6p(m=0)$ states, we have $\sigma(\varphi) = \text{const}$, and the phase space of electronic momenta is not weighted anymore with a transition probability. For the $6p(s)$ and $6p(a)$ states formed from the $6p(m=\pm 1)$ manifold, $\sigma(\varphi)$ can be simply deduced from the angular dependence of the orbitals:

$$\sigma_{6p(s)} = \cos\varphi/\sqrt{\pi},$$

$$\sigma_{6p(a)} = \sin\varphi/\sqrt{\pi}. \tag{6}$$

As compared to the 3D case, for the 2D case capture and loss rates become comparable so that one predicts much larger neutral fractions and, in particular, sizable populations of the Cs($6p$) manifold. In addition, the Fermi level for Cu(111) is close to the bottom of the surface-state continuum, $E_F - E_{SS} = 0.38$ eV. Thus, $k_F = 0.17$ a.u. is small, and the width of the kinematic resonance is clearly more narrow than in the 3D case.

Owing to the projected band gap of the Cu(111) surface, RCT rates are strongly reduced as compared to the case of projectile states in front of free-electron metal surfaces [18–21]. Under such conditions, other decay channels play a role. Recent studies on lifetimes of alkali-metal adsorbate-induced states on a Cu(111) surface have demonstrated the importance of inelastic electron-electron interactions for the decay of these states [20]. We use here the Fermi-liquid theory to estimate the multielectron contribution to the electron-loss rates [32,33]. Since the electron associated with a given quasistationary state of the projectile moves with average velocity $v_\parallel$ in the metal reference frame, its energy can be approximated by $E = E_i(Z) + v_\parallel^2/2$. Many-body contributions are added to the RCT decay rates in Eq. (5) according to

$$\Gamma_i^l(Z) \rightarrow G_i^l(Z) = \Gamma_i^l(Z) + A(Z) \frac{[\Phi + E_i(Z) + v_\parallel^2/2]^2}{[\Phi + E_{6s}(Z_{\rm ads})]^2}, \quad (7)$$

where $\Phi = 4.94$ eV is the work function of the target surface. $E_{6s}(Z_{\rm ads}) = -1.95$ eV is the energy with respect to the vacuum level of the Cs($6s$) resonance at an adsorption site with distance $Z_{\rm ads} = 3.5$ a.u. from the surface [20,34–37]. $A(Z)$ is given by

$$A(Z) = \Gamma_i(V_{\rm opt}, Z) - \Gamma_i(Z), \quad (8)$$

with $\Gamma_i(V_{\rm opt}, Z)$ being the total width of the state i which incorporates RCT and many-body contributions. This width is obtained from a WPP study where an optical potential $-iV_{\rm opt}$ was introduced inside the surface to account for the multielectron contributions in analogy with the low-energy electron-diffraction calculations [38]. $\Gamma_i(Z)$ is the total width of the state corresponding to the RCT process as given above. $V_{\rm opt} = 0.15$ eV is chosen in such a way that, for the static case, $A(Z_{\rm ads})$ reproduces the multielectron contributions to the width of the Cs($6s$) adsorbate resonance as obtained in an *ab initio* study [20] and confirmed by comparison with the time-resolved two-photon photoemission (TR-2PPE) data [34–37]. In addition, we have used $V_{\rm opt} = 0.25$ eV as could be deduced from the TR-2PPE studies of the excited electron dynamics in copper [32,33]. In order to justify the use of Eq. (7), we have explicitly checked in WPP calculations that $A(Z)$ scales linearly with $V_{\rm opt}$.

III. EXPERIMENT AND RESULTS

In our experiments we have scattered Cs^{q+} ions from an atomically clean and flat Cu(111) surface under a grazing angle of incidence of typically $\Phi_{\rm in} \sim 1°$. Since the key issue of the present study is based on the effect of the parallel-velocity component on charge transfer (parallel-velocity-assisted RCT), the projectile velocity has to be varied over a fairly high interval of velocities. Since Cs has a relatively high atomic mass, substantial projectile energies up to MeV have to be used for an appropriate tuning of the velocity in order to record the expected kinematic resonance structure for the neutral fractions in the scattered beam. The ions were produced in a Nanogan 10-GHz electron cyclotron resonance ion source mounted on a high-voltage platform, extracted with 10 keV, and accelerated by a voltage up to 100 keV. In order to obtain with our setup projectile energies in the MeV domain, ions with charge up to $q = 17$ were accelerated and scattered from the target surface.

The beam of Cs^{q+} ions was collimated by sets of slits in the sub-mrad domain. These slits also form components of two differential pumping stages in order to maintain a base pressure of some 10^{-11} mbar in the UHV target chamber against a pressure of typically 10^{-7} mbar in the accelerator beam line. The target was mounted on a precision manipulator and prepared by a fair number of cycles of grazing sputtering with 25-keV Ar^+ ions under a grazing angle $\Phi_{\rm in} \sim 2°$ and subsequent annealing at temperatures of about 520 °C. The state of preparation and the quality of the target surface was inspected by the width and structure of the angular distribution for scattered projectiles [26]. Fractions of the scattered beams could be selected by means of a narrow slit and were dispersed with respect to charge states by a pair of electric-field plates and detected by means of a channeltron detector.

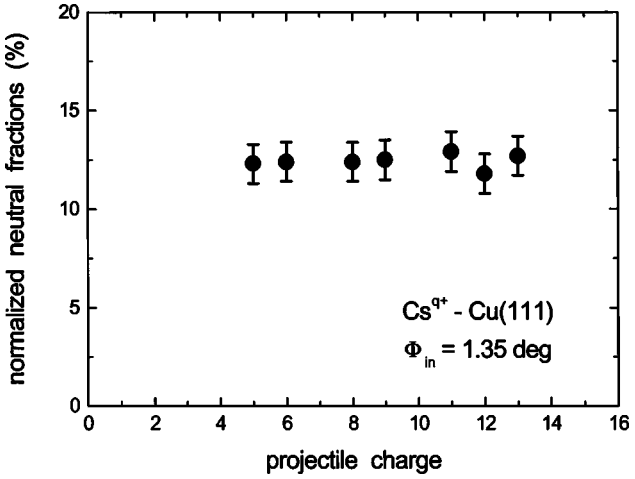

FIG. 1. Normalized neutral fractions as a function of projectile charge q for scattering of 525 keV Cs^{q+} ions from Cu(111) under $\Phi_{\rm in} \sim 1.35°$.

In our theoretical description of the RCT, we consider one-electron-transfer processes for the neutralization of incident ions via resonant neutralization or ionization of neutral atoms via resonant ionization. Thus, only neutral and singly ionized species in the scattered beam have to be taken into account in the analysis of data, i.e., we derive from the measured charge fractions normalized neutral fractions $P_o = n_o/(n_o + n_+)$, with n_o and n_+ being the charge fractions of neutral atoms and singly charged ions, respectively. In Fig. 1, we display normalized neutral fractions P_o for the scattering of 520-keV Cs^{q+} ions ($v = 0.39$ a.u., 1 a.u. = 1 atomic unit of velocity = Bohr velocity) from a Cu(111) surface under a grazing angle of incidence $\Phi_{\rm in} = 1.35°$ as a function of the charge q of the incident ions. We observe, within the experimental sensitivity of our experiment, no dependence of P_o on the charge of incident projectiles for $5 \leqslant q \leqslant 13$ (Fig. 1). This result demonstrates that the neutralization of the highly charged ions proceeds sufficiently fast and close to the surface in comparison with the final formation of atoms on the outgoing trajectory path. An important practical aspect of this observation results from the fact that owing to the high mass of Cs atoms (133 amu), high projectile energies up to MeV are needed in order to achieve velocities in the domain of atomic units (a.u.); the terminal voltage of our setup is limited to about 100 kV, so that high projectile energies can only be achieved here by making use of highly charged projectiles. Since Cs atoms have a fairly large number of weakly bound electrons of typically some tens of eV, the observation of a charge state equilibrium with respect to the final charge fractions is not surprising [39–41].

In Fig. 2, we show the dependence of the normalized neutral fractions as a function of the angle of incidence for specularly reflected projectiles. The data indicate a slight increase of P_o with increasing angle, i.e., RCT is affected by

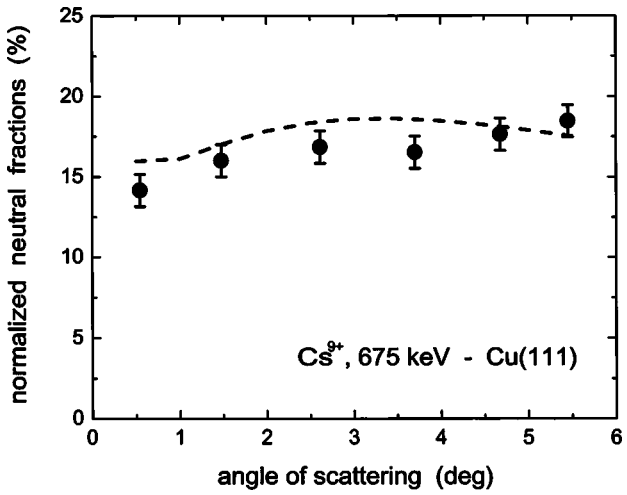

FIG. 2. Normalized neutral fractions as a function of angle of scattering for 675 keV Cs^{q+} ions reflected from Cu(111). The dashed curve represents results from our model calculations with $V_{opt}=0.25$ eV (cf. also Fig. 4).

the normal velocity component to a small amount only. This is confirmed by our calculations represented by the dashed curve, which reproduce the data fairly well (for details see below). A plot of P_o as a function of projectile velocity is presented in Fig. 3 for a grazing angle of incidence $\Phi_{in}=1.35°$. As we have mentioned, in order to achieve sufficiently high projectile velocities for the tuning of a kinematic resonance for the neutral fractions Cs^{q+} ions of charge up to $q=17$ have been used. The negligible effect of the charge of the incident projectile on the neutral fractions in the outgoing beam (cf. Fig. 1) is also reflected in these results which show, irrespective of the use of increasingly higher projectile charge for higher projectile velocities, a smooth curve revealing a kinematic resonance structure. These data are characterized by an onset at a velocity of about 0.15 a.u. and a broad peak where a structure is identified at lower velocities from the maximum. Based on model calculations, as detailed

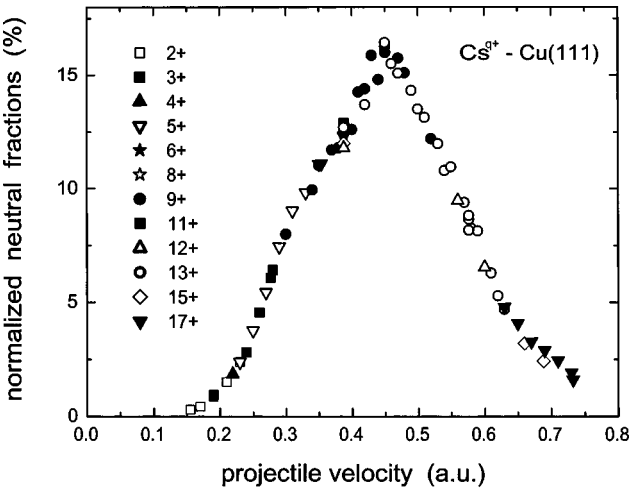

FIG. 3. Normalized neutral fractions as a function of projectile energy for scattering of Cs^{q+} ions from Cu(111) under $\Phi_{in}=1.35°$. Symbols represent the charge of incident projectiles.

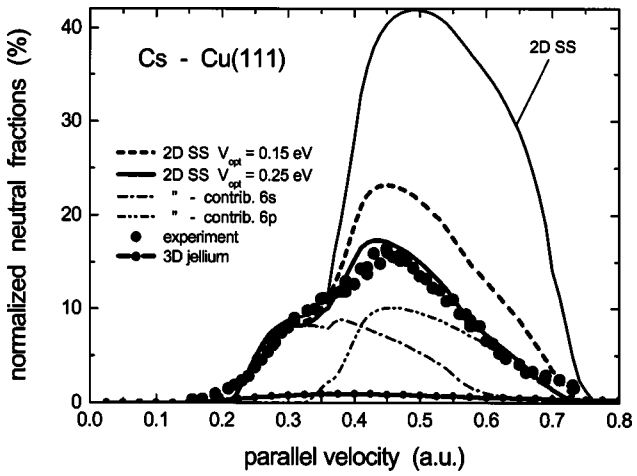

FIG. 4. Normalized neutral fractions as a function of projectile energy for scattering of Cs^{q+} ions from Cu(111) under $\Phi_{in}=1.35°$ (full circles). Solid curve with dots: calculations for the 3D continuum (jellium). Thin solid curve: calculations for the 2D surface-state continuum. Dashed and thick solid curve: calculations for the 2D surface-state continuum comprising optical potential with $V_{opt}=0.15$ eV and 0.25 eV, respectively. Dash dotted and dash dotted-dotted curves: contributions of $6s$ and $6p$ states to the total neutral fractions calculated for $V_{opt}=0.25$ eV.

in the preceding section, we will show below that this structure has its origin in pronounced contributions of excited levels to the final formation of Cs atoms.

IV. DISCUSSION

A crucial aspect of the effect of the projected band gap for the Cu(111) target on RCT is the dependence of the neutralization of Cs^+ ions on the (parallel) velocity. In the static case, the subject is simple. The Cs level has a clearly lower ionization energy than the target work function and, in addition, this energy is even further reduced by a shift owing to image charge effects [3]. As a consequence, RCT is completely dominated by resonant ionization, and contributions of electron capture are negligible. This feature is present in our data presented in Fig. 3 where a kind of threshold for the formation of neutral atoms can be identified, i.e., in the low-velocity limit our data consistently extrapolate towards a complete ionization of scattered projectiles. Thus, neutralization of projectiles can only proceed via a kinematically assisted RCT process, as observed previously for the scattering of a number of alkali-metal ions from a number of different metal targets [11,26,28].

The interesting feature of our work is related to the effect of the projected band gap and, in particular, the effect of the 2D surface-state continuum on the RCT process. The theoretical concepts were outlined in Sec. II. For comparison of theory and experiment, we have replotted in Fig. 4 the normalized neutral fractions shown in Fig. 3. The solid curve with circles termed ''3D jellium'' represents our calculations for RCT with the 3D continuum states of a free-electron metal with work function and Fermi energy for the Cu(111) surface. These calculations show a kinematic resonance

structure for P_o as a function of projectile velocity (more precise: parallel-velocity component; however, for grazing ion surface collisions the approximation $v_\parallel \simeq v$ holds better than 10^{-3}). The maximum of the calculated structure lies at $v=0.4$ a.u. which is about the same regime as observed in the experiment. Contributions of excited states in the calculations for a jellium target are found to be more than one order of magnitude smaller than for the ground state. A striking result of the comparison of these calculations with the data are experimental neutral fractions which are a factor of about 20 higher. This sheer contrast can hardly be attributed to general concepts in the theoretical description, since the same kind of theoretical approach provided excellent quantitative agreement with data obtained with, e.g., an Al(111) target, the prototype of a free-electron metal [11]. We therefore conclude that the observed discrepancy has to be ascribed to the specific electronic structure of the Cu(111) surface.

The thin solid curve in Fig. 4 represents calculations for RCT between projectile and 2D surface-state continuum which reproduce gross features of the experiment, however, the second peaked structure—attributed to the contributions of excited states to RCT ($6p$ states)—is clearly too large. The agreement between theory and experiment is significantly improved, if an enhancement of electron-loss rates due to multielectron effects is incorporated as outlined above. This results in the reduction of calculated neutral-atom fractions. The thick dashed and solid curves are results from calculations using $V_{\mathrm{opt}}=0.15$ eV and $V_{\mathrm{opt}}=0.25$ eV, respectively, where a quantitative agreement is achieved for the latter case.

We attribute the better agreement with data obtained with a higher amplitude of the optical potential to a partial correction of the deficiency in describing the band structure of the Cu(111) surface by the model potential used [23]. This potential is well suited close to the $\overline{\Gamma}$ point, but the description of the metal continuum gets poorer with increasing $k_\parallel$. The model potential imposes a free-electron-like dispersion of electronic states with momentum parallel to the surface: $E=E_i+k_\parallel^2/2m^*$ (effective mass $m^*=1$). This dispersion leads to the same projected band gap with increasing $k_\parallel$, and the surface state is always inside the band gap. On the other hand, photoemission studies show a dispersion of electronic states of Cu(111) with $k_\parallel$ that leads to a degeneracy of surface state and bulk states for $k_\parallel > 0.23$ a.u. [42]. Furthermore, the projected band gap closes at $k_\parallel \sim 0.63$ a.u. [43]. For grazing scattering, the electron is transferred from a projectile state to a state of the metal reference frame with $k_\parallel \sim v_\parallel$. Then with increasing $v_\parallel$ the ''effective'' Cu(111) band structure approaches the band structure of the free-electron metal concerning electron loss which should lead to an increase of electron-loss rates. As follows from Eq. (7), multielectron contributions to electron loss also increase with $v_\parallel$. With increasing optical potential, i.e., $A(Z)$, electron loss is enhanced for larger $v_\parallel$. We thus interpret the better quantitative agreement with the experimental data by using a higher amplitude of the optical potential by a compensation of deficiencies in the description of the band structure of Cu(111) by the model potential used. Note, however, that for projectile velocities $v<0.35$ a.u. quantitative agreement with the experimental data is achieved, whereas the calculated neutral fractions are not sensitive to a correction due to multielectron effects (the latter being small). This supports our interpretation of the experimental results in terms of a kinematically assisted RCT between projectile and 2D surface-state continuum and explains the problems with our theoretical approach at high velocities by the poor description of the dispersion of the Cu(111) states associated with the motion parallel to the surface.

Electron capture to higher excited states via kinematic effects can only proceed for projectile velocities clearly larger than those for population of the $6p$ manifold. This would correspond to the closing of the projected band gap as ''seen'' by electrons escaping from the projectile, and leads to a ''free-electron target'' behavior of electron loss. It is well established that the population of excited states in grazing scattering from the free-electron metals is very small [11,26–28]. This is, in particular, caused by large electron loss rates, so that we do not take into account $5d$ and higher states.

V. CONCLUSIONS

We have presented detailed studies on the neutralization of fast Cs ions during grazing scattering from a Cu(111) surface. Cs^{q+} ions of charge up to $q=17$ have been used in order to achieve sufficiently high projectile velocities for the tuning of a kinematic resonance for the neutral fractions. The negligible effect of the charge of the incident projectile on the neutralization probability shows that the equilibrium charge state is reached. The neutral fractions of specularly reflected beams reveal a resonance structure as a function of the projectile velocity which is attributed to a kinematically assisted RCT between the projectile and the target. As the most striking result we find neutralization probabilities an order of magnitude higher than that expected for a free-electron metal target surface. The enhanced neutralization probabilities are attributed to the effect of the projected band gap of the Cu(111) surface on resonant charge transfer. The measured neutral fractions can be consistently explained by the theoretical treatment incorporating the band-structure effects on the RCT using a model potential representation of the Cu(111) surface. A comparison between calculated and measured data reveals several important aspects, given in the following.

(1) Capture of electrons forming a 2D continuum of the surface state in the projected band gap of the Cu(111) surface plays a dominant role. This type of charge exchange enhances the electron capture in comparison to interactions with a 3D continuum.

(2) Enhancement of electron-capture probabilities holds, in particular, for excited $6p$ manifold of the projectile, so that these states have to be taken into account in a quantitative description of the experiments.

(3) The inelastic electron-electron interactions significantly contribute to the decay of the population of the projectile states, since RCT rates are strongly reduced as com-

pared to the case for a free-electron metal surface [18,19].

(4) For low projectile velocities, the experimental data are reproduced on a quantitative level by our approach free from adjustable parameters. The agreement between experiment and theory becomes poorer at higher projectile velocities, which we attribute to deficits of our surface model potential in view of a realistic Cu(111) band structure in a direction parallel to the surface.

The assistance of K. Maass and A. Schüller in the preparation and running of the experiments is gratefully acknowledged. This work was supported by the Deutsche Forschungsgemeinschaft (DFG, Grant No. Wi 1336).

[1] *Low Energy Ion-Surface Interactions*, edited by J. W. Rabalais (Wiley, New York, 1994).
[2] R. Brako and D. M. Newns, Rep. Prog. Phys. **52**, 655 (1989).
[3] J. Los and J. J. C. Geerlings, Phys. Rep. **190**, 133 (1990).
[4] J. Burgdörfer, in *Review of Fundamental Processes and Applications of Atoms and Ions*, edited by C. D. Lin (World Scientific, Singapore, 1993), p. 517.
[5] H. D. Hagstrum, Phys. Rev. **96**, 336 (1954).
[6] P. Nordlander and L. C. Tully, Phys. Rev. Lett. **61**, 990 (1988).
[7] D. Teillet-Billy and J. P. Gauyacq, Surf. Sci. **239**, 343 (1990).
[8] P. Kürpick and U. Thumm, Phys. Rev. A **54**, 1487 (1996).
[9] N. Lorente and R. Monreal, Surf. Sci. **370**, 324 (1997).
[10] M. A. Cazalilla *et al.*, Phys. Rev. B **58**, 13 991 (1998).
[11] A. G. Borisov, D. Teillet-Billy, J. P. Gauyacq, H. Winter, and G. Dierkes, Phys. Rev. B **54**, 17 166 (1996).
[12] J. N. M. van Wunnik, R. Brako, K. Makoshi, and D. M. Newns, Surf. Sci. **126**, 618 (1983).
[13] R. Zimny, Surf. Sci. **233**, 333 (1990).
[14] J. P. Gauyacq, A. G. Borisov, and H. Winter, Comments Mod. Phys. **2**, 29 (2000).
[15] L. Guillemot and V. A. Esaulov, Phys. Rev. Lett. **82**, 4552 (1999).
[16] T. Hecht, H. Winter, A. G. Borisov, J. P. Gauyacq, and A. K. Kazansky, Phys. Rev. Lett. **84**, 2517 (2000).
[17] T. Hecht, H. Winter, A. G. Borisov, J. P. Gauyacq, and A. K. Kazansky, Faraday Discuss. **117**, 27 (2000).
[18] A. G. Borisov, A. K. Kazansky, and J. P. Gauyacq, Phys. Rev. B **59**, 10 935 (1999).
[19] A. G. Borisov, A. K. Kazansky, and J. P. Gauyacq, Surf. Sci. **430**, 165 (1999).
[20] A. G. Borisov, J. P. Gauyacq, E. V. Chulkov, V. M. Silkin, and P. M. Echenique, Phys. Rev. B **65**, 235434 (2002).
[21] A. G. Borisov, J. P. Gauyacq, and S. V. Shabanov, Surf. Sci. **487**, 243 (2001).
[22] P. J. Jennings, R. O. Jones, and M. Weinert, Phys. Rev. B **37**, 6113 (1988).
[23] E. V. Chulkov, V. M. Silkin, and P. M. Echenique, Surf. Sci. **437**, 330 (1999).
[24] M. D. Feit and J. A. Fleck, Jr., J. Chem. Phys. **78**, 301 (1983).
[25] C. Leforestier *et al.*, J. Comput. Phys. **94**, 59 (1991).
[26] H. Winter, Phys. Rep. **367**, 387 (2002).
[27] E. R. Behringer, D. R. Andersson, B. H. Cooper, and J. B. Marston, Phys. Rev. B **54**, 14 780 (1996).
[28] J. N. M. van Wunnik and J. Los, Phys. Scr. **T6**, 27 (1986).
[29] E. G. Overbosch, B. Rasser, A. D. Tenner, and J. Los, Surf. Sci. **92**, 310 (1980).
[30] D. C. Langreth and P. Nordlander, Phys. Rev. B **43**, 2541 (1991).
[31] B. H. Cooper and E. R. Behringer, in *Low Energy Ion-Surface Interactions* (Ref. [1]).
[32] T. Hertel, E. Knoesel, M. Wolf, and G. Ertl, Phys. Rev. Lett. **76**, 535 (1996).
[33] R. Knorren, K. H. Bennemann, R. Burgermeister, and M. Aeschlimann, Phys. Rev. B **61**, 9427 (2000).
[34] H. Petek, M. J. Weida, H. Nagano, and S. Ogawa, Science **288**, 1402 (2000).
[35] S. Ogawa, H. Nagano, and H. Petek, Phys. Rev. Lett. **82**, 1931 (1999).
[36] M. Bauer, S. Pawlik, and M. Aeschlimann, Phys. Rev. B **55**, 10 040 (1997).
[37] M. Bauer, S. Pawlik, and M. Aeschlimann, Phys. Rev. B **60**, 5016 (1999).
[38] M. A. van Hove, W. H. Weinberg, and C. M. Chan, *Low Energy Electron Diffraction* (Springer, Berlin, 1986).
[39] S. T. de Zwart, T. Fried, U. Jellen, A. L. Boers, and A. G. Drentje, J. Phys. B **18**, L623 (1985).
[40] L. Folkerts, S. Schippers, D. M. Zehner, and F. W. Meyer, Phys. Rev. Lett. **75**, 983 (1995).
[41] C. Auth and H. Winter, Phys. Scr. **T92**, 35 (2001).
[42] S. L. Hulbert, P. D. Johnson, N. G. Stoffel, W. A. Royer, and N. V. Smith, Phys. Rev. B **31**, 6815 (1985).
[43] X. Guo *et al.*, Phys. Rev. B **57**, 6333 (1998).